University of Groningen

Langmuir-Blodgett films of amylose-esters and chiral azo-dyes

Schoondorp, Monique Annette

Publication date:
1992

CHAPTER 2

Structural study of Langmuir-Blodgett mono- and rnultilayers of amylose-esters with various alkyl chains.

SUMMARY

A series of amylose-esters with various side chain length was studied. Isotherms of the monolayers on the water surface were measured and polarized IR-measurements, SAXS-, and ellipsometric measurements were carried out in order to characterize the structure of the formed multilayers. Amylose-esters with short alkyl side chains appear to have a helical conformation on the water surface which can be transferred into multilayers. The amylose-palmitate ester however, as an example of an arnylose-ester with long alkyl side chains can only be transferred into rnultilayers when the degree of substitution (DS) is lower than about 2.3 and only then when the monolayer is in the liquid analogous state to some extent. Amylose-palmitate foms partly ordered Y-type multilayers with side-chains that have a preferential orientation perpendicular to the surface.

INTRODUCTION

Recently there was a renewed interest in the field of Langmuir-Blodgett(LB) films of preformed polymers, because of their degree of order and mechanical- and thermal stability [1,2,3]. The behaviour of some preformed polymers on the water surface was studied as early as 1924 [4], and later-on a systematic study of several polymers was carried out by Crisp [5]. Monolayer transfer of preformed polymers to form multilayers on a substrate was only studied in detail recently for some specific systems [6,7,8,9,10,11,12]. Initially, preformed polymers with distinct hydrophobic and hydrophilic parts, analogous to low molecular weight amphiphilic molecules were investigated. Tredgold has given a review on polymeric LB-materials other than

strictly amphiphilic [13]. It is known that poly(γ-methyl-L-glutamate), **poly(γ-benzyl-L-glutamate)** and copolymers of y-methyl-L-glutamate and **γ-benzyl-L-glutamate** form **LB-**multilayers built up with a-helices [14,15,16]. Strictly spoken, these helices are not **amphiphiles** but it seems that the ester linkages in the side-groups which point towards the water act as the hydrophilic moiety while the helix is sufficiently hydrophobic to prevent these materials from being soluble in water.

Kawaguchi et al. reported the formation of X-type **LB-films** of cellulose-esters with hydrophobic side groups [17,18]. These films appeared to be noncentrosymmetric and might be interesting for future applications in opto-electronic devices. However, LB-films of **cellulosetridodecanoate** could only be prepared with the horizontal lifting method. From structural study of the multilayers of these cellulose **tri-esters,** it was concluded that the glucose units with $\beta(1-4)$ linkages lie nearly flat on the water surface and the three vertical hydrocarbon chains attached to one glucose unit form a hexagonally packed ordered region. In the multilayer, the extended hydrocarbon chains are oriented perpendicular to the surface of the LB-film.

The difference between amylose-esters and cellulose-esters is the linkage between the **glucose-**units, an **α(1-4) linkage** in the case of an amylose-ester, a **β(1-4)** linkage in the case of a cellulose-ester. This different linkage has great influence on the molecular conformation.

In this paper we present a study of the monolayer properties of amylose-esters with short alkyl side chains (amylose-acetate, **-propionate** and **-butyrate),** medium length alkyl side chains (arnylose-laurate) and a long alkyl side chains (amylose-palmitate). Also the transfer of these esters using the vertical dipping method was studied. The structure of the LB-multilayers was determined by grazing incidence reflection (GIR) and transmission infrared spectroscopy, SAXS and **ellipsometry.** A comparison will be made with the known structure of the crystalline films of amylose-esters as studied by **Zugenmaier** and Steinmeier [19].

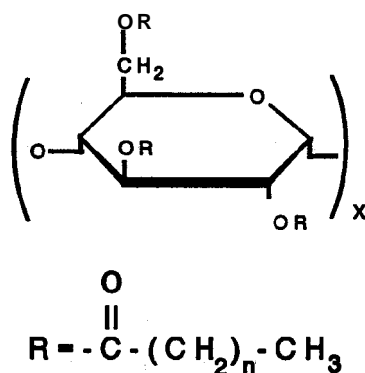## EXPERIMENTAL.

The amylose-esters used in this study were synthesized according to the method of Malm et al. [20] or to the **esterfication** method with N-methylimidazole as a reaction medium [21]. A high molecular weight sample amylose V from **Avebe** was hydrolyzed by dissolving the **amylose** in 10 wt.% **sodium** hydroxide at 90 °C. A 10 wt.% sulfuric acid solution was added until a pH of

1 was reached. This solution was stirred for 1 hour at 90 °C and cooled down to room temperature. The **residue** was washed with distilled water until a pH of 7 was reached and the product was dried. The **amylose** was hydrolyzed until a degree of polymerization of about 40 glucose-units based on DSC measurements.

Table 2.1 *Synthesized polymers.*

Polymer	n	Code	DS	Molecular weight repeating unit
Amylose-acetate	0	AAC	3.0	288
Amylose-propionate	1	APR	2.7	315
Amylose-butyrate	2	*AB*	2.7	353
Amylose-laurate	10	*AL*	2.6	643
Amylose-palmitate 1	14	AP1	1.7	574
Amylose-palmitate 2	14	AP2	2.3	721
Amylose-palmitate 3	14	AP3	3.0	877

Structural Formula.

$$R = -\overset{\text{O}}{\overset{\|}{C}} - (CH_2)_n - CH_3$$

Synthesis.

Amylose -acetate, -propionate, -butyrate and **-palmitate** 1 and 2 were synthesized by a one step procedure in N-methylimidazole.

Hydrolyzed **amylose** was dissolved in distilled N-methylimidazole at 90 °C with a concentration of 10 wt.%. The solution was cooled down to 5 °C and an excess of the corresponding

anhydride or acid chloride was added **dropwise** to the amylose solution. The reaction mixture was stirred for 4 hours at room temperature and the polymer was precipitated by pouring the mixture into methanol. The reaction product was purified two times by precipitation in methanol from chloroform solution **(p.a.quality)**. The degree of substitution (DS) was determined by elemental analysis. In order to prepare amylose-palmitate with a **DS = 3**, the above described procedure was followed twice. Amylose-laurate was synthesized according the method of Malm et al.[20] (see Table 2.1).

LB-films.

Monolayer properties were studied by pressure-area isotherms measured on a computer controlled **Lauda-Filmbalance** (FW 2) The **subphase** was purified water (doubly distilled followed by filtration through a Milli-Q purification system). The polymers were dissolved in chloroform (Uvasol quality) at concentrations of about 0.1 wt. %. Pressure-area diagrams were measured at different temperatures with a standard compression speed of 10 $Å^2$ molecular unit' min^{-1} . In order to elucidate the kinetic effects, isotherms were also measured at a lower speed (1 $Å^2$ molecular unit $^{-1}$ min $^{-1}$). ZnS-plates (Irtran, Spectra-tech), silicon wafers and gold layers on glass were used as substrates. The cleaning procedure of the silicon wafers was as follows: first the substrate was cleaned ultrasonically with chloroform and after drying it was treated with concentrated chromic acid for two hours at 80 °C, washed several times with Milli-Q water, washed ultrasonically with **aceton** and chloroform (all **p.a.** quality) dried and stored. Just before use, the substrate was rinsed with chloroform and partially hydrophobized by treatment of the substrates with a hexamethyldisilazane / chloroform solution (50 °C). ZnS-plates were ultrasonically cleaned with organic solvents. Gold substrates were prepared by sputtering gold (thickness of $\pm$ 500 Å) onto glass slides with a Biorad Turbo-coater E6700.

Transfer experiments were carried out after stabilization of the monolayer on the water surface at constant temperature and pressure.

FT-IR spectra.

All infrared measurements were carried out on a Bruker **IFS88** FTIR **spectro-photometer** with a MCT-A detector (D-313, Infrared Associates). The spectra were recorded with 4 cm^{-1} resolution. Grazing-incidence reflection spectra, with p-polarized light (perpendicular to the surface (E **1**)[22,23] were taken from multilayers on gold substrates. Transmission spectra with polarization parallel **to** the surface **(E//)** were obtained from multilayers deposited on both sides of a ZnS-plate of 2 mm thickness. The multilayer spectra were taken using 4 cycles of 250 scans each according to the method of Arndt et al. [24]. Transmission spectra with polarized

radiation (0" and 90") were obtained from the same multilayer. Spectra of isotropic samples of the polymers were obtained from films cast from chloroform solution onto KBr-disks. It was checked if this method gave isotropic spectra by comparing it with spectra measured from KBr-pellets.

RESULTS AND DISCUSSION

Monolayer properties

Figure **2.1** shows the pressure-area isotherms of the amylose-esters with a high DS ($>$ 2.6) with various alkyl chains at 24 °C. Amylose-esters with short alkyl side chains all show the same kind of behaviour (curve A, B and C, Fig. 2.1), only the areas per molecular unit where the transitions take place, differ. The laurate- and palmitate-ester show a completely different behaviour, which will be discussed further on.
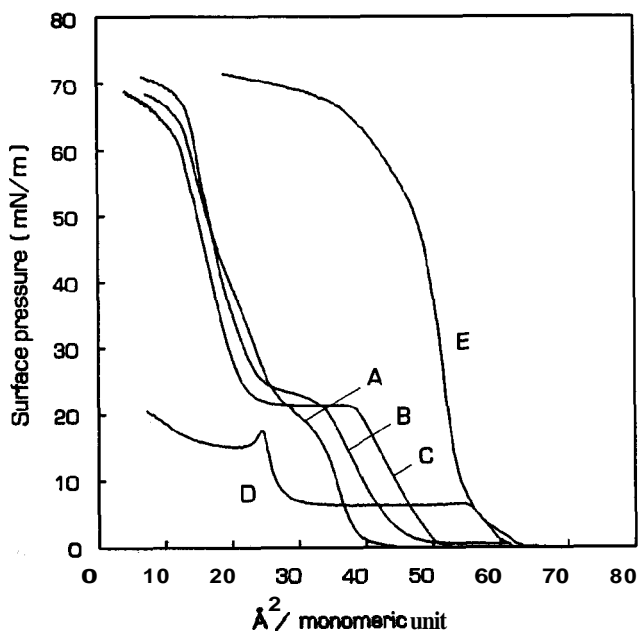

Figure 2.1 *Surface* pressure-area *isotherms* of amylose-esters with high DS at 24 °*C.* A = *Amylose-acetate,* B = Amylose-propionate, C = *Amylose-butyrate,* D = *Amylose-laurate,* E = Amylose-palmitate.

Figure 2.2 shows the temperature dependence of the isotherms of **AAC.** It appears that part of the isotherm ($\tau < 10$ **mN/m)** is independent of the temperature, whereas at higher surface pressure a considerable shift to lower area per monomeric unit occurs. The same effect was found for **APR** and **AB.** These isotherms were measured with a constant compression speed of $10 \, \text{Å}^2$ /monomeric unit $^{-1}$.**min** $^{-1}$ and additional **kinetic** effects might be present in these curves originating from slow processes in the monolayers.
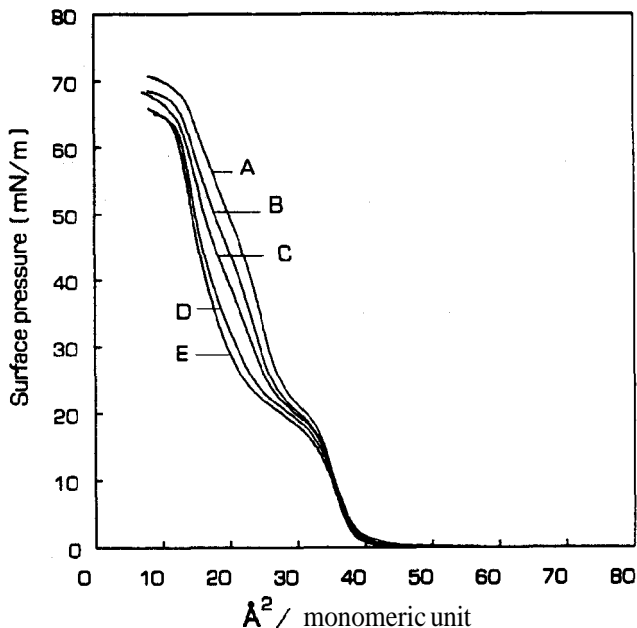

Figure *2.2   Temperature* **dependence** *of the surface pressure-area isotherms of amylose-acetate. A = 10.3 °C, B = 15.5 °C, C = 23.5 °C, D = 32.9 °C, E = 36.8 °C.*

In Figure 2.3 the effect of a lower compression speed on the isotherm of **AAC** is shown for two temperatures. Apparently at higher temperatures the effect of the compression speed is of minor importance, but at lower temperatures a pronounced effect can be seen on that part of the isotherm, which also shows a pronounced temperature dependence (curve **A** and B). From these two sets of experiments it can be concluded, that the isotherms of **AAC** (and also of APR and **AB**) can be divided in two parts. At low surface pressure the isotherm is independent of temperature and compression speed and is without kinetic effect and another part, where

considerable effects of both variables can be found, indicating that some kind of slow reorganization process may take place.
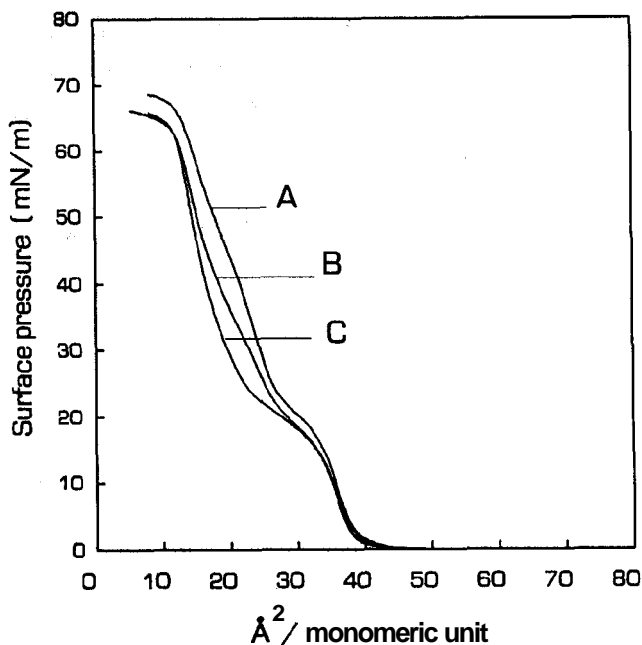

Figure *2.3* *Surface pressure-area isotherms of amylose-acetate with different compression speeds and temperatures. A = 15.5 °C and 10 Å² molecular unit⁻¹ min⁻¹., B = 15.5 °C and 1 Å² molecular* unit⁻¹ min⁻¹ *, C = 36.8 °C, 10 and 1 Å² molecular unit⁻¹ min⁻¹.*

More detailed information on both states can be found from stability experiments shown in Figure 2.4. For AB (and APR and AAC) a momentary stable layer is found at surface pressures < 10 mN/m, whereas at higher pressures (second part of the isotherms) a slowly decreasing area is found. However, after a rather long period also a stable state is found, which would not be expected if some kind of collapse process was taking place.

AAC forms a stable monolayer when the units occupy an area of 38 Å². The occupied area per molecular unit is reduced to almost half the original layer (22 Å²) after the transition that takes place at $\pi = 23$ mN/m.

Considering the glucose-unit as a three substituted flat ring the occupied area is in the range of 60 Å², as was found in the case of cellulose-esters, reported by Kawaguchi et al [17,18]

Zugenmaier and Steinmeier [19] determined the crystal structure of a homologous series of amylose-esters ranging from amylose-acetate to amylose-valerate by X-ray study, combined with conformational energy calculations. According to a conformational study of crystalline amylose-acetate , the amylose-acetate chain was proposed to have a conformation of a 9/7 helix with a rise per residue of 3.78 Å and a diameter of approximately **10 Å,** resulting in the value of 37.8 $Å^2$ per glucose-unit projected on a flat plane. This value agrees very well with the area found in the pressure-area curves in Fig. **2.1.**

Figure 2.4   *Stabilization of a mono- and bilayer at the air water surface at different surface pressures. Solid line (_____) is amylose butyrate, dashed line (- - - - -) is amylose laurate. A = 7 mN/m, B = 15mN/m, C = 23mN/m, D = 30 mN/m, E = 5mN/m, F = 7 mN/m and G = 11mN/m.*

Amylose-propionate (**APR**) and amylose-butyrate (**AB**) also form stable monolayers. When the pressure is raised to a surface pressure of **P** = 23 mN/m, also a transition takes place (Figure **2.1**). One esterified glucose-unit of **APR** occupies 47 $Å^2$ in a monolayer and **24 $Å^2$** after the transition. The values for the amylose-butyrate polymer are slightly higher: **51 $Å^2$** and **25 $Å^2$**

respectively. For the crystalline conformations it is calculated according to the data of Zugenmaier and Steinmeier that amylose-propionate occupies an area of 51 Å^2 when it is projected on a flat plane, for an amylose-butyrate helix this value is 57 Å^2, considering a 5/4 type helix with a rise per residue of 3.69 Å for both polymers.

We assume that the spread arnylose esters with short alkyl chains have the same helical conformation on the water surface as in the crystalline state. The discrepancy between the calculated values of the occupied areas for the glucose units and the value found in this study is probably due to experimental error. This is supported by the infrared spectra and the SAXS-data of the multilayers, discussed later on. In the isotherms of AAC, APR and AB there is a plateau region at a well defined surface pressure, where the monolayers clearly undergo a transition. It is thought that this transition corresponds with the transition from a monolayer to a bilayer. Malcolm has suggested this kind of transitions also for synthetic polypeptides . The plateau region is considered to be a regular collapse of the helices on the water surface to a more or less stable bilayer. The reduction of the area per residue after the transition to half the initial value supports this idea.

According to the theory of bilayer formation given by Malcolm , a number of molecules in a monolayer under pressure are forced out of the layer and act as nuclei for the formation of the second layer. Once this has happened, the second layer will be formed as a cooperative process due to attractive forces between the layers.

Figure **2.4** shows the formation of a monolayer and a bilayer of amylose-butyrate. The regions A and B (in Figure **2.4**) correspond to the formation of a stable monolayer. As can be seen, these monolayers are almost instantaneously stable. When the pressure in the monolayer is raised to the transition pressure (part C in Fig. **2.4**) the occupied area is reduced to half the initial area. At a pressure of **23 mN/m** (part C in Fig. **2.4**) the monolayer does not reach a complete stability in the shown time. The minimum decrease in occupied area per time unit in Figure 2.4 is determined at 0.13 mm /min. After at least 9 hours the layer reaches an equilibrium state. This behaviour is representative for the amylose-esters with the short alkyl chain. We could not find circumstances for transferring the more or less stable bilayer onto a solid substrate. Because the bilayer could not be transferred to a solid substrate the proposed structure is not confirmed by SAXS-, or ellipsometric measurements. Amylose-laurate is an example of an amylose-ester with a medium alkyl side chain. In order to investigate the monolayer properties of the laurate-ester the temperature dependence of the π-A isotherms was measured. Figure **2.5** shows the result of these measurements. The side chains have a liquid-analogous conformation at low

pressure (a < 10 mN/m), whereas above this pressure the side chains do no longer stabilize the monolayer and probably a phase transition takes place. The same kind of side chain behaviour is found for cellulose-laurate esters by Kawachuchi et al. [17,18].
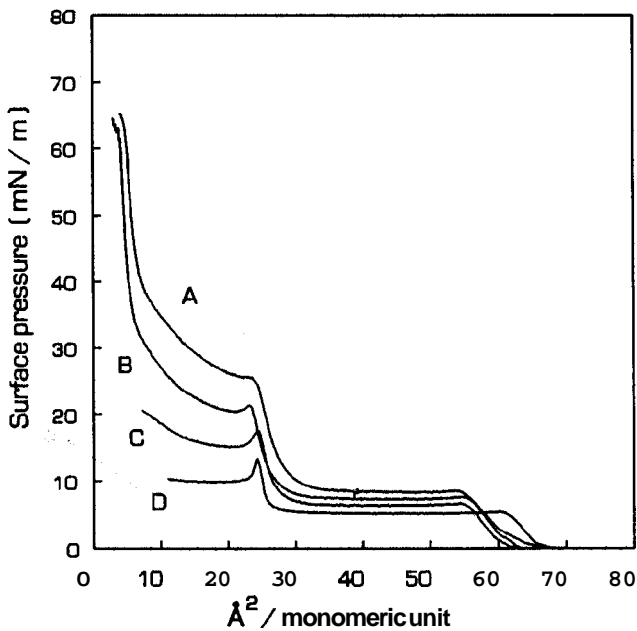

Figure 2.5   The temperature dependence of *surface* pressure-area *isotherms* of *amylose-laurate*. A = 10.8 °C, *B = 15.7 °C, C = 24.5 °C, D = 34.2 °C.*

The laurate-ester changes to a stable state, when the monolayer is coinpressed to an area of 25 $Å^2$ per unit as was verified by stabilization experiments like those in Figure 2.4. We assume that this transition corresponds to the formation of a helical bilayer like was found for the esters with short alkyl chains. Contrary to the amylose-esters with the short alkyl chains, the amylose-laurate polymer forms a completely stable layer at a pressure of 7 mN/m (part F in Fig.4) and 11 mN/m (part G in Fig.4) in a short time. The stability is probably enhanced by the increased attractive forces between the polymer chains of the amylose-laurate compared to the amylose-esters with the short alkyl chains at a low pressure. When the pressure is raised further, the more or less ordered layer collapses almost immediately because the medium alkyl chains do not have sufficient interaction with the water surface.

When the side chains are able to crystallize like in the amylose-palmitate polymer, the

monolayer behaviour is completely different as can be seen in Figure **2.6. At** low temperatures (T < 24 °C) there is no transition. When the molecules start to interact on a measurable scale, they form a condensed state with closely packed side chains. When the temperature is raised, the side chains are first in a liquid analogous state **and** upon increasing the pressure a transition takes place to the condensed state. One molecular unit that occupies $\pm$ 60 $Å^2$ corresponds with the area of a tri-substituted flat glucose ring and also to cross-sectional area of three vertical hydrocarbon chains. In order to elucidate the origin of the dimensions found for AP3 , isotherms of amylose-palmitate esters with different degrees of substitution were measured. From the isotherms (not shown) of **AP1,** AP2 and AP3 with a DS of 1.7, **2.3** and 3.0 respectively, the cross-sectional areas are determined. In the condensed state the extrapolated cross-sectional areas are **34 $Å^2$, 44 $Å^2$ and 58 $Å^2$** respectively. It can be deduced from these data that the value of the area of one molecular unit is controlled by the side chains. The cross-sectional area per substituted alkyl chain is found almost constant for the amylose-palmitate esters (19 $+$ 1 $Å^2$).
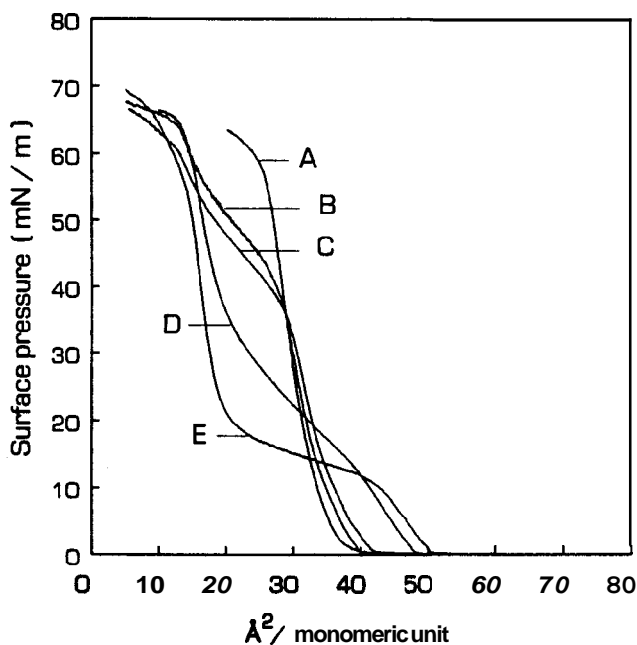

Figure 2.6   Temperature *dependence* of *surface* pressure-area *isotherms* of amylose-palmitate *(AP1).* A = *10.8* "C, B = *24.1 °C,* C = *25.8 °C, D* = 31.7 *°C,* E = *36.8* "C.

From the a-A isotherms we conclude that the monolayer properties of the arnylose-esters with short alkyl side-chains are mainly controlled by the backbone conformation. The behaviour of the isotherms of the medium and long chain amylose-esters is controlled by the side chains rather than the backbone.

Multilayers.

Formation of multilayers on partially hydrophobic substrates using the vertical dipping LB technique could be achieved with the amylose-esters with short alkyl side chains and with amylose-palmitate with a DS of 1.7 (AP1). Transfer ratios, the transferred monolayer area devided by the covered area of the substrate, were constant at least up to 50 layers under optimum conditions, as given in Table 2.11.

Table 2.II   Transfer properties of the amylose-esters.

Polymer code	Type of transfer	Transfer ratio ↓	Transfer ratio ↑	Temperature (°C)	Pressure (mN/m)
AAC	Z	0.0	1.0	22-28	7
APR	Y	0.7	1.0	25	10-15
AB	Y	0.7	1.0	25	12-18
AP1	Y	0.9	1.0	25-30	15-20

It is thought that the extent of hydrophilicity is responsible for the type of transfer [25]. Amylose-acetate is the most hydrophilic monolayer compared to the other amylose-esters used in this study and is the only polymer that gives Z-type transfer. With increased hydrophobic properties of the monolayer the transfer ratio on the down stroke increases, leading to more Y-type transfer. AP1 must exist to some extent in the liquid analogous state to realize constant deposition, as was found for other polymers [1,12,16]. For the higher substituted palmitate-esters it was not possible to find suitable transfer conditions. The closely packed alkyl chains, together with the stiff polymeric backbone apparently results in a rigid monolayer which prevents transfer. This phenomenon was studied in detail for various poly-octadecylmethacrylates[26].

Table 2.III *IR-band assignments.*

Vibration (cm^{-1})	M	AAC	APR	AB	AP1
ν_a (CH$_3$)	] C-CH$_3$	2956	2962	2965	2957
ν_a (CH$_2$)	⊥ C-C-C		2946	2937	2932
ν_s (CH$_3$)	‖ C-CH$_3$		2878	2878	
ν_s (CH$_2$)	‖ H-C-H				2852
ν_s (C=O)	‖ C=O	1749	1745	1745	1744
δ_a (CH$_2$)	‖ C-C-C		1463	1461	1465
δ_a (CH$_3$)	‖ C-C-C	1432			
δ_s (CH$_2$)			1421	1416	1413
δ_s (CH$_3$)		1371	1380	1382	1377
Coupled motions of C-O-C (ester groups)			1272	1250	1237
		1237	1175	1171	1164
Coupled motions of glucose units and linkages		1165	1165	1090	1115
		1128	1087		1085
		1036	1036	1035	1030

Structural measurements.

Bulk FT-IR spectra of an isotropic sample were compared with GIR spectra and transmission spectra of the multilayers. For GIR spectra it is known that individual group vibrations, inducing dipole moment changes of this group, absorb strongly when these dipole moment changes are oriented perpendicular to the reflecting metal mirror [22,23]. Correspondingly they will not absorb in the transmission spectra of the same structure, where the electric field vector of the light is parallel to the substrate. Orientation of the molecules might also be deduced from transmission spectra obtained with polarized IR light, for instance perpendicular and parallel to the dipping direction. To our knowledge no detailed vibrational analysis of the amylose-esters has appeared in the literature. Band assignments have to be made by combining the results of other

compounds.

Comparing the FT-IR spectra of amylose-acetate with the afore mentioned different modes, differences can be seen if the bulk spectrum of AAC (film on KBr-disc) is compared to the GIR-spectrum of AAC in the region **1200 cm^{-1} - 800 cm^{-1}**. Comparison of the GIR-spectrum of AAC with the bulk spectrum cannot be done directly because of dispersion effects which are present in the GIR-spectrum [27].
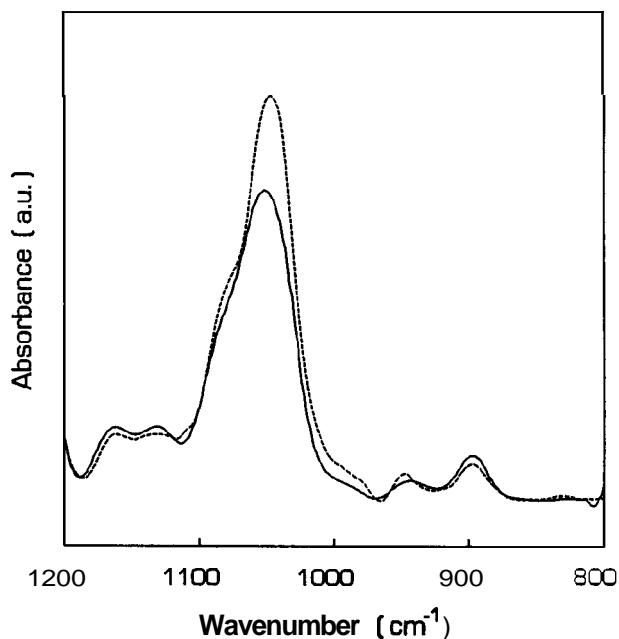

Figure 2.7A *IR-spectra of amylose-acetate. Solid line (___) GIR-spectrum of 15 LB-multilayers on a gold substrate. Dashed line (- - -) calculated GIR-spectrum of a bulk sample of amylose-acetate.*

Figure 2.7A shows the calculated bulk spectrum of AAC in the GIR mode and the actually measured GIR-spectrum.

The GIR bulk spectrum is calculated using the matrix formalism of Abèles [28]. The optical constants are calculated using the KBr-spectrum of AAC of known thickness, a mean refractive index of **1.48** and the Kramer-Konig relationship [29]. The thickness of the KBr spectrum is calculated from the measured interference fringes of free standing AAC films. The orientation of AAC can be found in the absorption band at **1036 cm^{-1}**, which is ascribed to a C-O-C

vibration mode. However, this C-O-C bond is present in the glucose-ring as well as outside the glucose-ring as a connecting link between the glucose-units. From a detailed investigation of the vibration spectra of pure **amylose** [30] it was concluded that the region below the 1500 cm^{-1} is complex with coupled vibration modes, and therefore it is impossible to draw any definite wnclusions about the precise orientations of the polymer chains in the LB-layers. No orientation effects were found in the vibration absorbances above 1200 cm^{-1}.
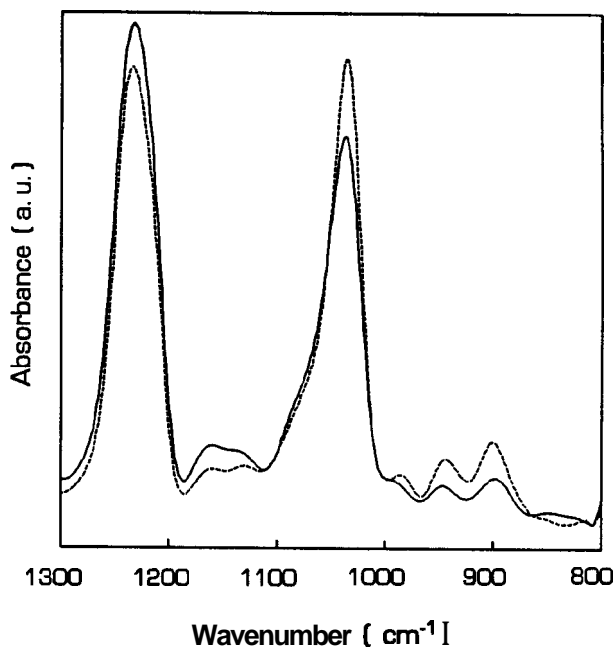

Figure 2.7B *Transmission spectra of LB-layers consisting of 15 monolayers of amylose-acetate on each side of a ZnS plate. Solid line (_____) polarized light perpendicular to the dipping direction. Dashed line (- - -)polarized light parallel to the dipping direction.*

Figure 2.7B shows the transmission spectra of AAC on Irtran-2 substrates with two different polarizations of the IR beam. Distinct differences can be seen between two spectra in the 1300 - 800 cm^{-1} region. The other part of the spectra did not show any changes. From this we may conclude that in these LB-multilayers orientation of the polymer molecules occurs, whereas the orientation of the ester side chains is not found because in all cases the absorption of the C=O

group at 1749 cm^{-1} remained constant. From these polarized transmission spectra it follows that there is an orientation of the polymer backbone towards the dipping direction. The dichroic measurements agree with the idea of the helical conformation of the amylose-acetate in the LB-layers. In a helical conformation a dichroic effect can only be expected when the absorbing vibration is **fixed** in the conformation. Freely rotating groups are expected to have a random distribution. Comparing the GIR-spectrum with the transmission spectrum using light polarized perpendicular to the dipping direction , the absorption at 1036 cm^{-1} changes in the same way. This can be explained by the suggested model of oriented helices. Both spectra detect the helices from the same point of view, namely perpendicular to the helix axis. Moreover, the same IR dichroic results were obtained by just uniaxial stretching of a bulk amylose-acetate film. The amylose-propionate polymer and the amylose-butyrate polymer show the same tendency in the dichroic spectra as the amylose-acetate polymer. Polarized transmission IR-measurements of the propionate and butyrate polymer did not show any preferential orientation, which is probably due to the incomplete down-stroke transfer (Table 2.11).

In Figure 2.8A the grazing angle spectra of 15 LB-multilayers of amylose-palmitate (AP1) before (___) and after heating (- - -) are shown. For comparison the KBr bulk spectrum is given (B). The dispersion of the refractive index had no measurable effect on the reflection spectrum as was calculated.

Of particular interest in these spectra is the CH_2 stretching region (3000 - 2800 cm^{-1}). The stretching vibrations ν_a (CH_2) at 2957 cm^{-1} , ν_a (CH_2) at 2932 cm^{-1} and ν_s (CH_2) at 2852 cm^{-1} show a decrease of about 47 percent in the GIR spectrum co'mpared to the bulk spectrum. After heating the sample for 16 hours at 120 °C the GIR spectrum changes to the dashed line in Fig. 8A . This spectrum coincides with the bulk spectrum B indicating that the original orientation of the molecules completely disappeared. From these measurements it follows that the CH_2 chains of the amylose-palmitate polymer have a preferential orientation perpendicular to the substrate, which disappears upon heating. Contrary to the amylose-esters with short alkylchain-esters, where only the absorption bands of the C-O-C vibrations deviate in the dichroic spectra, almost **all** bands in the amylose-palmitate polymer deviate from the bulk spectrum. This indicates that also the glucose ring has a specific orientation. Transmission spectra with different polarizations of the IR-beam are shown in Fig. 2.8B. The most striking difference between the polarizations perpendicular (_____) and parallel (- - -) to the dipping direction are the ring breathing vibrations at 945 cm^{-1} and 905 cm^{-1}. Also the C-O-C bands show some dichroic effect. From these spectra it follows that there might be a small orientation of the backbone of
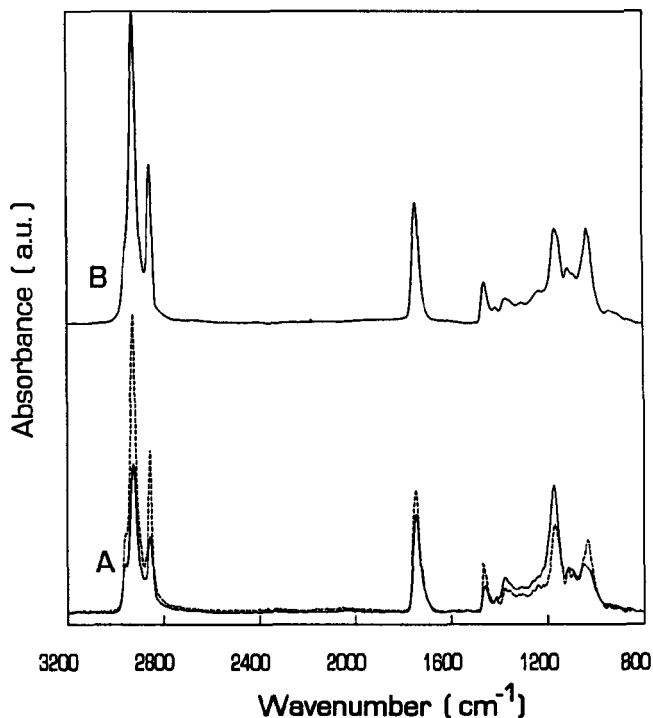
the molecule in the dipping direction.

Figure **2.8A** *IR-spectra of amylose-palmitate. A (solid line)* = *GIR-spectrum of*
15 layers of arnylose-palmitate on a gold substrate as deposited. A (dashed line)
= *GIR-spectrum of the same multilayer as A after heating 16 hours at 120 °C.*
B = *KBr bulk spectrum.*

Multilayers of amylose-esters with short alkyl chains do not show any reflection in the **SAXS**-experiments. Because of this absence of reflections in the **SAXS** experiments ellipsometric measurements were carried out to determine the thickness of the layers of the amylose-esters. The results are given in Table 2.IV. The thicknesses appear to agree reasonably well with the estimated diameter of the corresponding crystalline helices when the incomplete transfer of APR and AB is also taken into account. The calculated thickness of one layer varies a little with the total thickness of the layer as can be seen in Table 2.IV. This can not be explained by irregular transfer. At this moment we can not give a suitable explanation.
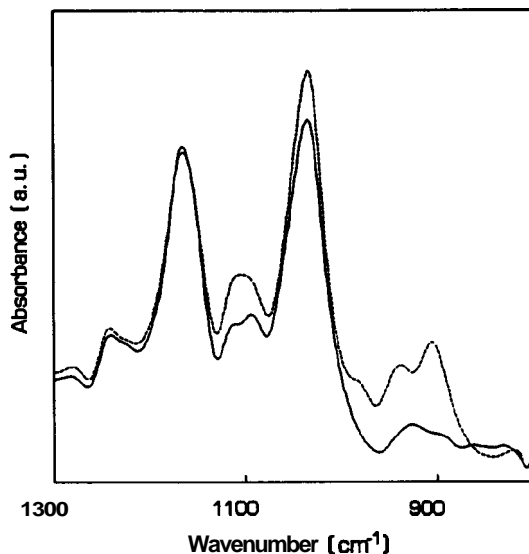
*Figure 2.8B Transmission IR-spectra of amylose-palmitate. Solid line (_____) = 15 LB-multilayers on each **side** of a **ZnS plate**, with polarized light perpendicular to the dipping direction. Dashed line (- - -) = 15 **LB-multilayers** on both sides of a ZnS plate with polarized **light** parallel to the dipping direction.*

Table 2.IV *Thickness of the **multilayers** of the **amylose-esters** with **short alkyl** side chains.*

Polymer	Number of layers	Transfer ↓	Transfer ↑	Total thickness (Å)	Thickness one layer (Å)	Crystalline thickness[a]
AAC	15	0	1.0	136±4	9.1	10.1
	20	0	1.0	184±2	9.2	
APR	20	0.7	1.0	202±2	11.8	10.8
	36	0.7	1.0	304±8	9,9	
AB	20	0.7	1.0	208±4	12.2	11.8
	40	0.7	1.0	387±9	11.4	
AP1	40	0.9	1.0	836±9	22.0	-

[a] Average thickness of one helix in the crystalline unit cell, as computed by Zugenmaier and Steinmeier[19].

SAXS experiments of **amylose-palmitate** multilayers do not show any reflections either. From **ellipsometric** measurements the thickness of one layer was determined to be **22 Å**. This value corresponds almost to stretched **CH₂** chain of **15** C-atoms. **A** fully stretched chain has a length of **19 Å.** This result corresponds with the IR data, although the layer is not regular enough to give X-ray reflections. The lack of X-ray reflections may arise from the fact that the multilayers are prepared by transferring monolayers in the liquid analogous state.

Finally the results are combined in Figure **2.9,** showing a schematic representation of the proposed structure of the LB-Nms of the amylose-esters with the short **alkyl** chains and the long **alkyl** chains.
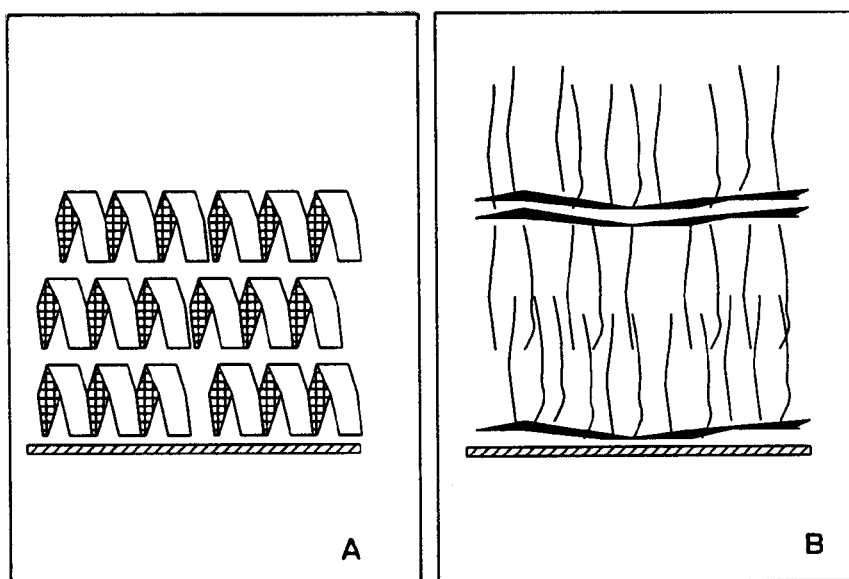

Figure 29 *Schematic* representation of the proposed structure of the LB-films.
A = *LB-film* of amylose-esters with short alkyl *chains.* B = LB-film of *amylose-*esters with long alkyl chains.

CONCLUSIONS.

Monolayer properties of a series of amylose-alkylesters were studied and it was found that amylose-esters with short alkyl side chains form helices on the water surface. The dimensions of the helices on the water surface agree with the corresponding crystalline polymers reported by Zugenmaier et al.[19]. A transition from a stable monolayer to a bilayer was observed. The monolayer properties of the amylose-esters with medium and long alkyl side chains were controlled by the side chains rather than by the backbone. The side chains of the amylose-laurate polymer were not able to crystallize. In contrast to the laurate-ester, the palmitate side chains do crystallize on the water surface causing a condensed state. **Multilayers** of amylose-acetate, - propionate, **-butyrate** and the palmitate with a DS of 1.7 could be prepared at least up to 50 monolayers. The amylose-acetate polymer formed Z-type layers with a transfer ratio of unity and the helical conformation is conserved in the multilayer. Moreover a preferential orientation of the helices parallel to the dipping direction could be deduced from the dichroic IR spectra. The other polymers showed more or less Y-type transfer.

Polarized IR measurements and X-ray diffraction of the amylose-palmitate polymer revealed a more or less ordered structure with a preferential orientation of the alkyl chains perpendicular to the surface.

REFERENCES

1. Duda,G., Schouten,A.J., Arndt,T., Schmidt,G.F., Wegner,G. *Thin Solid Films,* 1988, *159,* 221.

2. Biddle,M.B., Lando,J.B., Ringsdorf,H., Schmidt,G., Scheider,J. *Colloid. Pol. Sci.* 1988, 266, 806.

3. Watanabe,M., Kosaka,Y., Oguchi,K., Sanui,K., Ogata,N. *Macromolecules* 1988, 21, 2997.

4. Katz,J.R., Samwell,P.J.P., *Ann. Chem.* 1924, *472,* 241.

5. Crisp,D.J. *J. Coll. Sci.* **1946**, *1,* 161.

6. Tredgold,R.H., Winter,C.S. *J.Phys. D.* **1982**, *15*, L55

7. Tredgold,R.H., Winter,C.S., *Thin Solid Films* 1983, *99,* 81.

8.   Mumby,S.J., Swalen,J.D., Rabolt,J.F. Macromolecules 1986, 19, 1054.

9.   Elbert,R., Laschewsky,A., Ringsdorf,H. J. Am. Chem. *Soc.* 1985, 107, 4134.

10.   Schneider,J., Ringsdorf,H., Rabolt,J.F. Macromolecules, 1989, 22, 205.

11.   Schneider,J., Erdelen,C., Ringsdorf,H., Raolt,J.F. Macromolecules, 1989, 22, 3474.

12.   Schouten,A.J., Wegner,G. Makromol. Chem., 1991, 192, 2203.

13.   Tredgold,R.H. Thin Solid Films 1987, 152, 223.

14.   Malcolm,B.J. Proc. R. *Soc.* London, Ser. A., 1968, 305, 363.

15.   Winter,C.S., Tredgold,R.H. Thin Solid Films 1985, 123, L1.

16.   Duda,G. *Ph.D.* Thesis, Mainz 1988.

17.   Kawaguchi,T., Nakahara,H., Fukuda,K. Thin Solid Films, 1985, 133, 29.

18.   Kawaguchi,T., Nakahara,H., Fukuda,K. J. Colloid. Int. *Sci.* 1985, 104, 209.

19.   Zugenmaier,P., Steinmeier,H. Polymer, 1986, 27, 1601.

20.   Malm,C.J., Mensch,J.W., Kendal,D.L., Hiatt.G.D. *Ind.* Eng. Chem., 1951, 43, 684.

21.   Wachwiak,R., Conners,K.A. Anal. Chem., 1979, 51, 27.

22.   Greenler,R.G. J. Chem. Phys. 1966, 44, 310.

23.   Arndt,T. Ph. D. Thesis. Mainz **1988**.

24.   Arndt,T., Bubeck,C., Schouten,A.J., Wegner,G. *Mikrochim. Acta*, 1988, 11, 7.

25.   Popovitz-Biro,R., Hill,K., Lahav,E.M., Leiserowitz,L., Sagiv,J., Hsiing,H., Merendith,G.R., Vanherzeele,H. J. Am. Chem. *Soc.* 1988, 110, 2672.

26.   Arndt,T., Schouten,A.J., Schmidt,G.F., Wegner,G. Makromol. Chem., 1991, 192, 2215.

27.   Graf,R.T., Koenig,J.J.L., Ishida,H.H. Pol. Prep.,1984, 25, 188.

28.   Abèles,F. Ann. Phys., 1948, 12, 33.

29.   Allara,D.L., Baca,A., Pryde,C.A. Macromolecules, 1978, 11, 1215.

30.   Mthlouthi,M., Koenig,J.L. *Adv.* in Carbon Chemistry and Biochemistry, Academic Press, Orlando FL, 1986, **Vol.44**, p.7.